Ab initio thermodynamics of oxide surfaces: O_2 on $Fe_2O_3(0001)$

Wolfgang Bergermayer and Hannes Schweiger
Institut Supérieur des Matériaux et Mécaniques Avancés, 72000 Le Mans, France

Erich Wimmer*
Materials Design, Angel Fire, New Mexico and Le Mans, France

(Received 22 October 2003; revised manuscript received 23 February 2004; published 20 May 2004)

The oxygen coverage, structure, and thermodynamic stability of (0001) surfaces of Fe_2O_3 (hematite) as a function of temperature and oxygen pressure are investigated by *ab initio* density functional theory with the generalized gradient approximation. Spin-polarized total energy and force calculations are performed using the projector augmented wave method as implemented in the Vienna *ab initio* simulation package. At high chemical potentials of oxygen (i.e., high pressure or low temperature), the most stable (0001) surface of hematite is completely covered with oxygen atoms. At low chemical potentials, a structure with one surface iron atom per two-dimensional unit cell is found to be the most stable surface termination. Around 800 K at an oxygen partial pressure of 0.2 bar, this reactive surface iron atom can bind and release an oxygen atom, thus switching between formal oxidation states (III) and (V), i.e., between stoichiometric and ferrate-like states. The fully reduced (iron terminated) surface is found to be thermodynamically unstable and dissociates adsorbed oxygen molecules spontaneously.

DOI: 10.1103/PhysRevB.69.195409 PACS number(s): 68.35.Bs

I. INTRODUCTION

Metal oxides offer a fascinating range of unique physical and chemical properties, which render this class of materials extremely important scientifically and technologically. One of the intriguing properties of many oxides is their catalytic activity, which has corollaries in sensors, corrosion, and environmental degradation of metals and alloys. Despite this obvious importance and the long history of oxide-based technologies, many fundamental issues related to oxides are still unresolved or not understood in detail. In particular, our knowledge of oxide surfaces is rather limited due to the experimental difficulties in preparing and characterizing such surfaces. This lack of knowledge represents a serious hindrance to further progress, especially in view of emerging nano-technologies, where stringent control of materials and their surfaces is crucial. Thus, there is an urgent need to deepen our understanding of metal oxides and their surfaces based on a detailed characterization and analysis on the atomic scale.

In this context, the present work focuses on a prototypical metal oxide, namely iron oxide in the form of hematite (Fe_2O_3). Specifically, we address chemical composition, structure, and thermodynamic stability of the dominant (0001) surface of this oxide as a function of the partial pressure of molecular oxygen in the gas phase and the temperature of the system. Furthermore, we investigate the related question of the structure and energetics of chemisorbed molecular oxygen on $Fe_2O_3(0001)$ surfaces.

Our approach is based on spin-polarized density functional theory (DFT)[1–4] using the generalized gradient approximation (GGA)[5,6] for describing electronic exchange and correlation effects. The Kohn–Sham equations are solved with a plane wave basis as implemented in the Vienna *ab initio* simulation package (VASP)[7–9] with its projector augmented wave (PAW) potentials.[10,11]

Electronic structure calculations on iron oxide surfaces are confronted with serious challenges due to the existence of various oxidation states of iron, the localized character of $3d$-electrons leading to strong correlation effects, the importance of magnetic effects, and the structural complexity of hematite. For these reasons, the first *ab initio* calculations on iron oxides surfaces are fairly recent.[12,13]

The applicability of the present approach to the iron–oxygen system was tested for the structure and energetics of bulk FeO (wüstite), bulk α-Fe_2O_3 (hematite), and the diatomic molecule FeO. The rationale for this validation is the concern that the GGA within DFT may lead to unacceptable errors due to the electronic structure of iron oxide, which can be referred to as ''highly-correlated system.'' A necessary condition for the applicability of the DFT-GGA level of theory is its ability to predict bond distances within a few percent of experiment. This can be readily tested for bulk iron oxides and molecules such as FeO. It is found that the errors are within the typical range of this level of theory, thus justifying its application to iron oxide surfaces.

The central part of the present work is a detailed investigation of different terminations of the $Fe_2O_3(0001)$ surface and the relationship between surface stability, oxygen pressure, and temperature. Compared with the structures discussed by Wang *et al.*,[12] a new particular ''ferrate-like'' surface structure is identified, which involves a tetrahedrally coordinated Fe atom in a formal oxidation state of $+5$. This ferrate-like structure is predicted to be stable in a range of temperature and oxygen pressure close to the thermodynamic conditions applied, for example, in the industrial catalytic oxidation of ethylbenzene to styrene. Therefore, this structure is believed to be important in understanding the catalytic properties of iron oxides. In addition to the study of the different surface terminations, the interaction with oxygen was investigated for the first time. We give a detailed description of the structure and energetics of chemisorbed mo-

lecular oxygen on the most important $Fe_2O_3(0001)$ surfaces.

II. THERMODYNAMIC APPROACH

Conceptually, the physical system of the present study consists of three regions, namely a large region of bulk hematite with the stoichiometry Fe_2O_3, a large gas phase region consisting of molecular oxygen at pressure P, and a surface region with chemical composition Fe_xO_y in an *a priori* unknown structure and stoichiometry. The surface region contains a total number of N_{Fe} and N_O of iron and oxygen atoms, respectively. The entire system is surrounded by a thermal bath of temperature T. The oxygen partial pressure and the temperature are kept in a range where hematite is thermodynamically stable, i.e., the oxygen partial pressure is sufficiently high and the temperature sufficiently low.

At thermodynamic equilibrium of this solid–gas interface, for all species the respective chemical potentials are equal in each region. For the iron atoms in the system, the large region of bulk hematite determines their chemical potential. The chemical potential of oxygen is given by its value in the molecular gas of pressure P and temperature T. Therefore, the free energy, Ω, of a hematite surface under an oxygen atmosphere can be written as

$$\Omega = G - N_{Fe}\mu_{Fe} - N_O\mu_O, \tag{1}$$

where G is the Gibbs free energy of the surface region, $N_{Fe}\mu_{Fe}$ is the Gibbs free energy of all iron atoms in the surface region with a chemical potential of Fe equal to that in bulk hematite, and $N_O\mu_O$ is the total Gibbs free energy of all oxygen atoms in the surface region with a chemical potential equal to that in the gas phase. For a given temperature and pressure, the thermodynamically most stable system minimizes its surface free energy by adapting the stoichiometry of the surface region, i.e., by varying N_{Fe} and N_O. Conceptually, this is accomplished by an exchange of Fe atoms from the large region of bulk Fe_2O_3 and the surface region and by exchanging O atoms between the solid and the gas phase.

For $P_O=0$ and $T=0$ with a slab model for the surface and $G\cong E$, Eq. (1) leads to the familiar expression for surface energies, namely

$$\gamma = \frac{1}{2A}(E_{slab} - E_{bulk}), \tag{2}$$

where γ is the surface energy, E_{slab} is the total energy of the slab, E_{bulk} is the total energy of the bulk system with the same number of atoms as in the slab, and A is the surface area of the unit cell.

To see the connection between Eqs. (1) and (2), one can use the following steps: (i) the Gibbs free energy $G=E_{el}+E_{vib}+E_{other,internal}+PV\text{-}TS$ is approximated by the electronic energy, E_{el}, which is often the dominant term; (ii) the surface region is replaced by a single slab with the stoichiometry of the bulk phase. The Gibbs free energy of the surface region is then approximately $G\cong E_{el,slab}$; (iii) with the stoichiometry given above and the constraint that the chemical potential of each species is equal to that of the species in the bulk, the term $N_{Fe}\mu_{Fe}+N_O\mu_O=G_{bulk}\cong E_{el,bulk}$. Setting $\Omega = A\gamma$, normalizing by the surface areas A, and taking into account the fact that a slab has two surfaces, Eq. (1) becomes Eq. (2). For a more detailed discussion of surface thermodynamics we refer to the book by Zangwill.[14]

The Gibbs free energy of the surface region is given by

$$G = E + PV - TS \tag{3}$$

with E being the internal energy. It is assumed that the terms PV and TS are similar for different surface terminations and thus can be canceled. Furthermore, the internal energy E is approximated by the total electronic energy, E_{el}, of the surface region as obtained from ground state electronic structure calculations. This assumption implies that the phonon density of states of the solid does not depend strongly on the surface structure and composition. In particular, one assumes that the zero-point energies of the various systems are similar and thus can be ignored. Obviously, these are approximations which need to be kept in mind in the analysis of the results.

The chemical potentials of Fe and O, μ_{Fe} and μ_O, are connected through bulk Fe_2O_3, which serves as reservoir of Fe atoms. Thus, we have

$$2\mu_{Fe} + 3\mu_O = \mu^{bulk}_{Fe_2O_3}, \tag{4}$$

where $\mu^{bulk}_{Fe_2O_3}$ is the chemical potential of bulk Fe_2O_3. This term is approximated by the total electronic energy per formula unit of bulk α-Fe_2O_3.

With these assumptions and approximations, one obtains

$$\Omega = E_{slab} - \tfrac{1}{2}N_{Fe}\mu^{bulk}_{Fe_2O_3} + (\tfrac{3}{2}N_{Fe} - N_O)\mu_O. \tag{5}$$

Division by the surface area per unit cell, A, and accounting for the two surfaces of the slab leads to the surface free energy

$$\gamma = \frac{\Omega}{2A}. \tag{6}$$

The gas phase above the iron oxide surface contains molecular oxygen. It is assumed that the pressure is sufficiently low and the temperature sufficiently high so that one can neglect intermolecular interactions and treat the pressure dependence as ideal gas. Therefore, the chemical potential of oxygen, μ_O, as a function of temperature and oxygen partial pressure is given by

$$\mu_O(T,P) = \mu_O(T,P^0) + \frac{1}{2}kT\ln\left(\frac{P}{P^0}\right). \tag{7}$$

The temperature dependence of the chemical potential of molecular oxygen contains the vibrational and rotational degrees of freedom. In principle, this could be obtained from *ab initio* calculations. However, following common practice, the temperature dependence of μ_O is taken from experimental data as given in standard thermodynamic tables[15] (cf. Table I).

As reference for the chemical potential of an oxygen molecule at $T=0$ and $P=0$ we take $\mu_O(T=0,P=0) = \frac{1}{2}E^{total}_{O_2} = -4.909$ eV, i.e., half of the total energy of a spin polar-

TABLE I. Experimental temperature dependence of the chemical potential of molecular oxygen, $\mu_O(T,P^0)$ at a pressure of $P^0 = 1$ bar (after Ref. 15).

Temperature (K)	Chemical potential (eV)
100	−0.08
200	−0.17
300	−0.27
400	−0.38
500	−0.50
600	−0.61
700	−0.73
800	−0.85
900	−0.98
1000	−1.10
1100	−1.23
1200	−1.36
1300	−1.49
1400	−1.62
1500	−1.75

ized oxygen molecule using the same supercell and computational approach as for the surface calculations (cf. Sec. IV). Thus, all terms of Eq. (5) are defined and one can study the dependence of the surface free energy as a function of the chemical potential of oxygen (i.e., of oxygen pressure and temperature) for a set of different surface models. In this way, a (P,T) phase diagram of the Fe_2O_3 surface can be established.

It is reasonable to restrict the range of the chemical potential of oxygen by the conditions that (i) hematite does not decompose forming bulk iron and (ii) molecular oxygen does not condense on the surface. These conditions imply

$$\mu_{Fe} < \mu_{Fe}^{bulk}, \tag{8}$$

which is equal to

$$\mu_O > \tfrac{1}{3}(\mu_{Fe_2O_3}^{bulk} - 2\mu_{Fe}^{bulk}) \tag{9}$$

for the lower limit of the oxygen chemical potential. Actually, the lower limit for the oxygen chemical potential is somewhat higher, because hematite, upon reduction, first transforms into magnetite, then changes to wüstite before finally becoming pure iron.

The condition for the upper limit is

$$\mu_O < \frac{1}{2} E_{O_2}^{total}. \tag{10}$$

Using the computed total energies for bulk Fe, bulk Fe_2O_3, as well as the total energy of molecular O_2, we obtain the boundaries in (eV)

$$-2.3\text{eV} < \mu' = \mu_O - \tfrac{1}{2} E_{O_2}^{total} < 0. \tag{11}$$

III. STRUCTURAL MODELS

The most common form of Fe(III) oxide is α-Fe_2O_3, which is known under the mineralogical name hematite. This mineral crystallizes in the corundum structure in space group $R\bar{3}c$. It can be interpreted as a hexagonal close-packed structure of slightly distorted oxygen ions with 2/3 of the intersti-

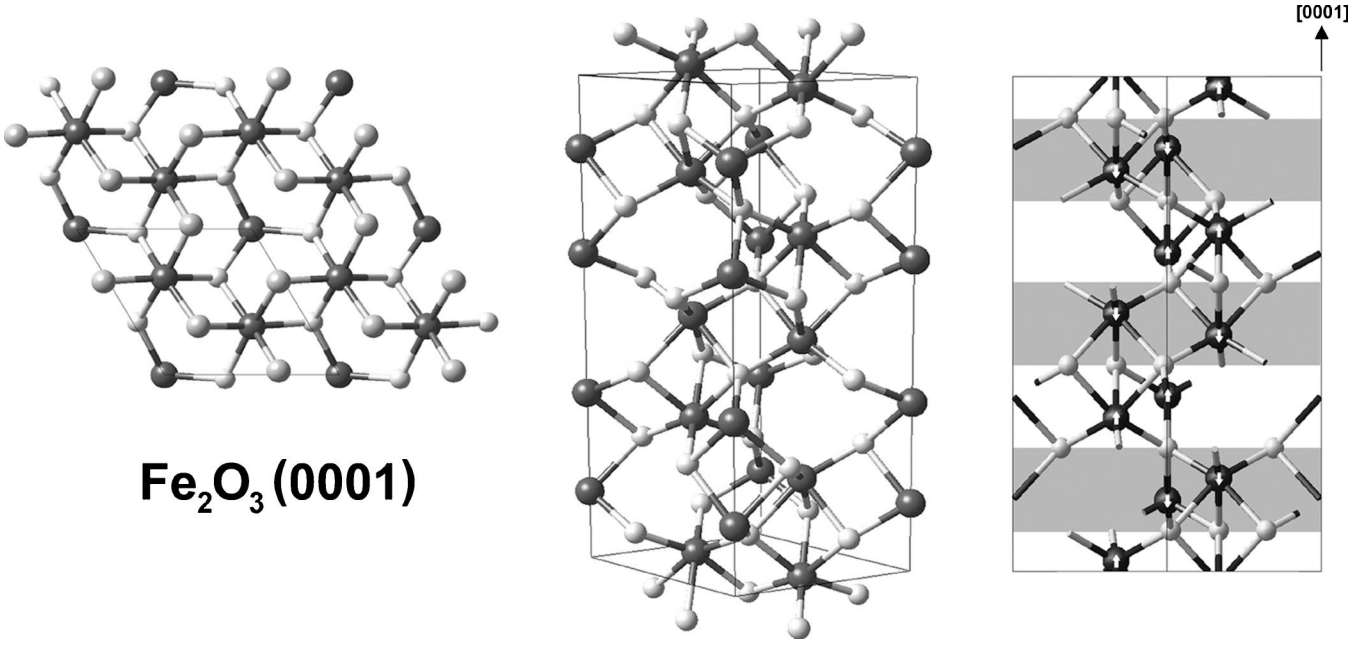

FIG. 1. Structure of hexagonal α-Fe_2O_3 (hematite). The left panel shows a top view of the (0001) surface terminated by a layer of oxygen atoms, the central panels gives a perspective view, and the right panel is an orthogonal view parallel to the (0001) planes. The oxygen atoms (light gray spheres) form a slightly distorted hexagonal close-packed structure with three atoms per layer (per unit cell). The iron atoms (dark spheres) occupy octahedral sites with two atoms per layer. Each of the gray and white bands contains exactly one Fe_2O_3 formula unit and is thus charge neutral. The arrows indicate magnetic ordering of the low-energy antiferromagnetic state.

TABLE II. Lattice parameters and total energies of hexagonal α-Fe_2O_3. NM denotes a nonmagnetic calculation, FM and AFM represent ferromagnetic and antiferromagnetic ordering, respectively. The two AFM spin arrangements refer to the ordering in the Fe layers as explained in the text.

	Expt.[a]	Wang *et al.*[a]	NM	FM ↑↑↑↑↑↑↑↑	AFM′ ↑↓↑↓↑↓↑↓	AFM ↑↑↓↓↑↑↓↓
$a=b$ (Å)	5.035	5.025	4.711	4.779	5.029	4.995
c (Å)	13.747	13.671	13.625	13.298	13.852	13.858
E_{el} (eV)			−223.041	−224.574	−224.854	−227.358
ΔE (eV)			4.317	2.784	2.504	0.000

[a]Reference 12.

tial octahedral sites being occupied by Fe ions.[16] Along the [0001] direction of hematite, two iron layers alternate with slightly distorted hexagonally close-packed layers of three oxygen atoms per unit cell (cf. Fig. 1). Following the nomenclature of Wang *et al.*,[12] we can write this structure as $-Fe-Fe-O_3-Fe-Fe-O_3-$.

The (0001) surface is stable at ambient temperature and oxygen partial pressure and shows no reconstruction.[16,17] According to Weiss and Ranke,[13] this is also a catalytically active surface. Starting from bulk α-Fe_2O_3 and maintaining the two-dimensional periodicity of the conventional unit cell, there are the following possibilities to create (0001) surfaces: $O_3-Fe-Fe-O_3$, $O_2-Fe-Fe-O_3$, $O_1-Fe-Fe-O_3$, $Fe-Fe-O_3$, and finally $Fe-O_3$. These five surface terminations have been investigated by Wang *et al.*[12]

There is an additional surface termination, denoted $O-Fe-O_3$, which has not been analyzed so far. As will be shown in the following, this is the energetically preferred structure in an important range of temperature and oxygen pressure and thus may play an important role in the catalytic properties of this system.

All of these six different surface structures have been investigated in the present calculations. The surfaces are represented by a repeated-slab model containing on average 12 atomic layers. The spacing between the slabs is approximately 15 Å. The model is constructed such that inversion symmetry is maintained, i.e., both surfaces of the slab are identical. Using the computed lattice parameters in the direction parallel to the (0001) surface as obtained from bulk calculations, the atomic positions of all atoms in the slab are fully relaxed, resulting in optimized geometries and corresponding total energies as discussed in the following.

The thermodynamic stability of the various iron oxide surfaces as a function of temperature and oxygen partial pressure is derived from the condition of equal chemical potential of oxygen in the gas phase and at the surface as discussed in the previous section.

IV. COMPUTATIONAL ASPECTS

The computation of the ground state structures is based on spin density functional theory[1–4] using the generalized gradient approximation (GGA) for the exchange–correlation potential.[5,6] The Kohn–Sham one-particle wave functions are expanded in a plane wave basis with projector augmented wave (PAW) potentials[10] as implemented by Kresse and Joubert.[11] The PAW potential for Fe is constructed for eight valence electrons of the configuration $3d^74s^1$ and the O potential for six valence electrons with the configuration $2s^22p^4$. This PAW approach contains the physical aspects of an all-electron, frozen core method, while maintaining the computational efficiency of pure plane wave methods. The cut-off in the plane wave expansion was 400 eV. All calculations were performed with the Vienna *ab initio* Simulation Package (VASP)[7–9] within the MedeA technology platform.[18]

The computations were performed in several stages concerning the geometry optimizations and the k meshes. When calculating surfaces or adsorption on iron oxide surfaces, it was found to be advantageous to relax the surface atoms layer by layer while fixing the rest of the system in order to obtain good convergence. Toward the end of the convergence process, all atoms are relaxed. In terms of the k-space integration, the initial stages of the calculations used a $2\times2\times1$ Monkhorst-Pack k-mesh, which was increased to a $4\times4\times1$ k-mesh in the final stages close to geometric convergence.

In order to study the influence of spin polarization on the results, both magnetic and nonmagnetic calculations were performed. Given the complex magnetic structure of iron oxides, full optimizations of the cell parameters and internal coordinates were carried out for bulk Fe_2O_3 in different arrangements of the magnetic moments, as will be discussed in the following.

V. RESULTS

A. Validation for FeO and bulk Fe_2O_3

As an initial step, the applicability of the GGA within spin-polarized DFT was probed for FeO (wüstite), which crystallizes in the NaCl structure and thus can be computed very rapidly. An optimization of the cubic cell with a non-spin-polarized Hamiltonian leads to a lattice parameter of 4.09 Å, which is about 5% smaller than the experimental value[19] of 4.312 Å. A spin-polarized calculation for a ferromagnetic ordering results in a theoretical value of 4.32 Å, i.e., there is a change of about 6% in the lattice parameter between nonmagnetic and magnetic calculations. These results clearly demonstrate the importance of magnetic effects on the structural parameters of iron oxides.

As the next step, the lattice parameters of the hexagonal α-Fe_2O_3 bulk unit cell were optimized using nonmagnetic,

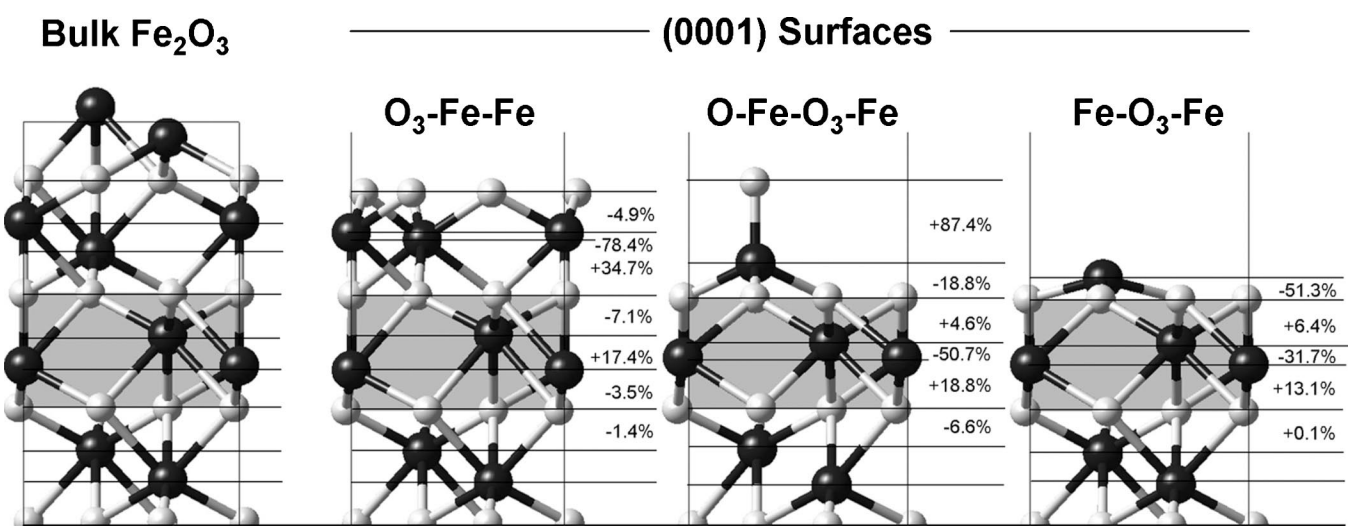

FIG. 2. Structure and relaxation of the most relevant Fe_2O_3 (0001) surface terminations as a function of oxygen coverage. All values are relative to the corresponding interlayer spacing in bulk Fe_2O_3. Regions of charge neutrality are shaded. Note the pronounced flattening of the subsurface Fe double-layer in the case of the fully oxidized surface denoted O_3–Fe–Fe with a similar tendency for the cases O–Fe–O_3–Fe and Fe–O_3–Fe.

ferromagnetic and antiferromagnetic arrangements of the spin. Regarding the antiferromagnetic ordering, two different spin configurations were investigated, namely one with parallel spins within each iron double layer but antiparallel to the next double layer, and one with antiparallel spins within each double layer. The results are given in Table II.

As in the case of wüstite, the nonmagnetic calculation seriously underestimates the lattice constants of hematite. The differences in the lattice parameters obtained from ferromagnetic (FM) and antiferromagnetic (AFM) calculations demonstrate the importance of the ordering of the spin moments. In the FM case, the lattice parameters deviate strongly from experiment and the total energy is about 2.8 eV per cell higher compared with the ground state. The lattice parameters from both AFM models are in good agreement with experiment. However, there is a pronounced difference in the total energy between the two AFM cases. The configuration with parallel spin within each double iron layer (taken as energy reference in Table II) is energetically favored by 2.5 eV per cell compared to the case of antiparallel spin within a double layer. Therefore, the model with parallel spins in each double layer and AFM ordering between the double layers represents the ground state within the present approach and therefore will be used for all further calculations (cf. Fig. 1). This ordering is consistent with the experimental fact that hematite is an antiferromagnet with a Néel temperature of 955 K. (Below 260 K hematite becomes a weak ferromagnet. This low-temperature transition is due to subtle effects of noncollinear magnetism, which are not considered in the present context.) The bulk-like structure of α-Fe_2O_3 is maintained also in thin films, as discussed by Schedel-Niedrig *et al.*[16]

The deviation of the lattice parameters from the experimental values is about 0.8% for a and c. These are reasonable results lying well within the usual errors of the GGA method.

The diatomic molecule FeO represents another limiting test case. A geometry optimization of this molecule in a large

TABLE III. Surface relaxations (in % relative to the interplanar spacing in bulk α-Fe_2O_3) of the different terminations for the Fe_2O_3(0001) surface compared with the FLAPW results of Wang *et al.*[a] For surface terminations, where several geometries are possible (e.g., O_2–Fe–Fe and Fe–O_3–Fe), only the energetically most favorable geometry is listed.

	Ref. (12) O3–Fe–Fe 16 L	O3–Fe–Fe 16 L	O2–Fe–Fe 16 L	O1–Fe–F– 16 L	Fe–Fe–O3 14 L	Ref. (12) Fe–O3–Fe 18 L	Fe–O3–Fe 12 L	O–Fe–O3–Fe 14L
Fe–O3						−57	−51.3	−18.8
O3(/2/1)–Fe	−1	−4.9	4.9	5.5		7	6.4	4.6
Fe–Fe	−79	−78.4	−56.3	−26.3	8.0	−33	−31.7	−50.7
Fe–O3	+37	34.7	14.6	−5.7	−46.7	15	13.1	18.8
O3–Fe	−6	−7.1	3.5	7.4	23.7			
Fe–Fe	+16	17.4	7.6	4.3	−4.4			
Fe–O3	−4	−3.5	−4.6	−5.2	−5.1			

[a]Reference 12.

TABLE IV. Magnetic moments (in μ_B) for $Fe_2O_3(0001)$ surfaces with various terminations as described in the text.

	O3–Fe–Fe 16 L	O2–Fe–Fe 16 L	O1–Fe–Fe 16 L	Fe–Fe–O3 14 L	Fe–O3 12 L	O–Fe–O3 14L
O	0.2	0.2	0.3			0.1
Fe–Fe	1.7	2.8	3.4	3.1	3.3	1.4
O3	0.1	0.0	0.0	0.0	0.0	0.0
Fe–Fe	−3.6	−3.5	−3.5	−3.5	−3.5	−2.4, −3.3
O3	0.0	0.0	0.0	0.0	0.0	0.0

supercell using the same level of theory as applied in the above bulk calculations gives a bond length of 1.62 Å with a magnetic moment of 4 μ_B, which corresponds to a quintet ground state. This is in excellent agreement with the experimental bond length of 1.6259 Å for the $^5\Sigma^+$ state of the diatomic molecule.[20–22]

Given that spin polarized DFT with the GGA gives reasonable bond distances and magnetic ordering in bulk iron oxides and the diatomic molecule FeO consistent with the usual errors of GGA calculations, one can assume that this level of theory may also give meaningful structural and total-energy related information for the surfaces of iron oxides, which represent intermediate cases between the two limits of a bulk solid and molecules. However, the calculation of properties such as photoemission spectra and pressure-induced metal-insulator phase transitions of Fe_2O_3 requires a different level of theory such as LDA+U and there may also be consequences for the character of the frontier orbitals.[23] Nevertheless, the results obtained for the test cases discussed in this section provide evidence that the DFT-GGA level of theory is meaningful for the prediction of overall structural and energetic properties of the Fe–O system.

B. $Fe_2O_3(0001)$ surfaces

We will now focus on the different surface terminations of $Fe_2O_3(0001)$ starting with the fully oxidized O_3–Fe–Fe surface. This system shows a very strong relaxation, as can be seen from Fig. 2 and Table III. The main effect is a strong inward displacement of the surface atoms resulting in a flattening of the double layer of iron atoms below the surface oxygen atoms (cf. Fig. 2). Adopting the notation of Wang *et al.*,[12] this relaxation can be described as a contraction of about 5% between the oxygen layer and the iron layer, and a contraction of as much as 78% between the two iron layers. In addition, the distance to the oxide layer below is enlarged by about 35%. The relaxation even affects deeper layers, such that the distance within the next Fe–Fe double layer is widened by 17%. These values are in very good agreement with the FLAPW results of Wang.[12] Clearly, surface relaxation plays an important role for this material.

Proceeding from the system O_3–Fe–Fe, we gradually reduce the surface by removing oxygen. There are several possibilities of abstracting an oxygen atom from the O_3–Fe–Fe surface to create an O_2–Fe–Fe termination. Within the present model, all cases were investigated and the energetically most stable arrangement is given in Table III. Again, we see a strong contraction between the outermost Fe–Fe double layer, and a widening of the distances between the Fe and O_3 layers below, although somewhat more moderate than in the case of O_3–Fe–Fe termination. This trend continues as another oxygen atom is removed from the surface. In the case of the O_1–Fe–Fe surface, there is still a contraction of 26% within the Fe–Fe double layer. The widening to the underlying O_3 layer reverses to a contraction of about 6%.

For the fully reduced Fe–Fe–O_3 surface, the relaxation is of different sign: in this case, there is a widening of 8% within the Fe–Fe double layer, and a contraction of 47% between the Fe and O_3 layers. The distance of the O_3 layer to the underlying Fe layer is enlarged by 24%. Thus, the fully oxidized and fully reduced surfaces show different geometric characteristics in terms of relaxation. This is likely to be related to the charge distribution in the different surface terminations. In the case of O_3–Fe–Fe, there is a stoichiometric excess of 1.5 oxygen atoms in the surface layer (cf. Fig. 2). In the system O_2–Fe–Fe, the excess is only 0.5 oxygen atoms and in O_1–Fe–Fe, there is a stoichiometric deficiency of 0.5 oxygen atoms in the surface layer.

The next step is the removal of one of the Fe atoms, which results in a surface termination with a single Fe layer. Among the different possible locations of the surface Fe

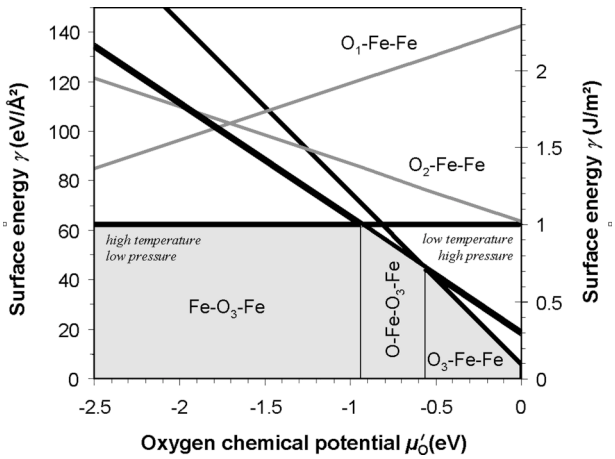

FIG. 3. Free energy of a Fe_2O_3 (0001) surface as a function of oxygen chemical potential. The thermodynamically stable structures are Fe–O_3–Fe, O–Fe–O_3–Fe, and O_3–Fe–Fe. Within the valid range of μ_O, the surfaces O_2–Fe–Fe and O_1–Fe–Fe are metastable.

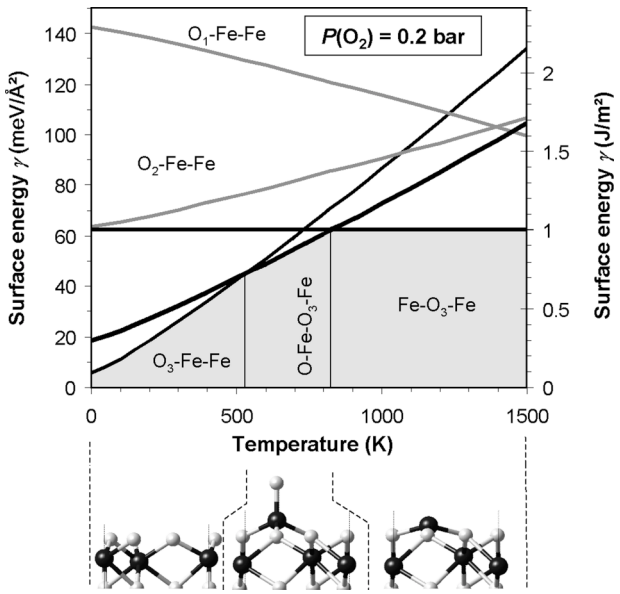

FIG. 4. Free energy of a Fe_2O_3 (0001) surface as a function of temperature for a constant oxygen partial pressure of $P(O_2) = 0.2$ bar. The thermodynamically stable structures Fe–O_3–Fe, O–Fe–O_3–Fe, and O_3–Fe–Fe are shown at the bottom.

atom, the most stable arrangement is one with the Fe atom in the position equivalent to the bulk stacking. One finds a strong contraction of -51% between this single Fe layer and the O_3 layer, whereas the other relaxations are similar to the O_3 terminated case (contraction between Fe–Fe double layer and widening to the underlying O_3 layer). The surface layer is perfectly stoichiometric (cf. Fig. 2), namely $FeO_{1.5}$ or Fe_2O_3 and the nominal oxidation state of this type of surface iron atom is $+3$.

All of these surfaces can be directly created by cleavage of bulk Fe_2O_3. If one considers an oxygen-rich environment, there is another possible surface termination, namely an oxidation of the Fe–O_3–Fe surface to O–Fe–O_3–Fe. This surface termination was not mentioned by Wang *et al.*, but it has recently been discussed by Surnev *et al.*[24] in the context of surface terminations of metal oxides crystallizing in the corundum structure. In this geometry, an O atom forms a bond to the surface Fe atom with a bond length of 1.6 Å, thereby reducing the bonding between the Fe atom and the O_3 layer. The relaxation of the surface iron atom toward the underlying O_3 layer becomes less pronounced by changing from -51.3% to -18.8%. The subsurface relaxations show the same tendency as for the Fe–O_3–Fe surface, but are slightly enhanced.

The surface Fe atoms in the O–Fe–O_3 case have a formal oxidation state of $+5$ and a tetrahedral coordination of oxygen atoms. Such a coordination is known for this high oxidation state of iron in ferrate compounds such as $K_3(FeO_4)$.[25]

The magnetic moments of the various terminations of the Fe_2O_3(0001) surface are summarized in Table IV. In the interior of the slab, the moments remain close to their bulk values of about 3.5 μ_B for the Fe atoms and 0.0 μ_B for O. At the surface, the magnetic moments of the Fe atoms are reduced considerably if the surface is terminated by oxygen atoms. The surface oxygen atoms show a small magnetic moment of 0.2–0.3 μ_B, whereas the moment on the surface Fe atoms lies between 1.7 μ_B in the fully oxidized case, 2.8 μ_B in the presence of two O atoms, and 3.4 μ_B if there is only one O atom present. In the case of the Fe terminated surface, be it an iron double layer or single layer, the magnetic moments of the Fe atoms remain in the range between 3.1 and 3.3 μ_B. Thus, adsorption of oxygen atoms reduces the magnetic moments of the surface Fe atoms. One should keep in mind that the DFT-GGA level of theory underestimates the absolute value of magnetic moments in Fe_2O_3 and that theories such as LDA+U are needed to obtain quantitative agreement in the magnetic moments.[23]

C. Thermodynamic stability of Fe_2O_3(0001) surfaces

Using the thermodynamic approach described in Sec. II, the stability of various stoichiometric compositions of Fe_2O_3(0001) surfaces is obtained as a function of the chemical potential of oxygen as shown in Fig. 3. At high chemical potentials of oxygen, i.e., at low temperatures or high partial pressures of oxygen, the fully oxygen-covered O_3–Fe–Fe surface is thermodynamically the most stable termination. At the other limit, namely at a low chemical potential of oxygen (high temperatures or low oxygen pressures), the reduced Fe–O_3–Fe surface is stable. In the range of the oxygen chemical potential between -1 and -0.5 eV, the most stable surface is the Fe(V) ferrate-like surface termination O–Fe–O_3–Fe. The surfaces O_2–Fe–Fe and O_1–Fe–Fe are unstable in the entire viable range of oxygen chemical potentials.

The transition from Fe–O_3–Fe to O–Fe–O_3–Fe at $\mu' = -0.9$ eV is intuitively very appealing. It means that the Fe_2O_3(0001) surface features reactive Fe atoms, which are able to capture and release oxygen atoms at intermediate temperature and pressure conditions, thus shuttling between Fe(III) and Fe(V) oxidation states. The oxygen atoms are sterically easily accessible and thus may play a key role in catalytic redox reactions on this surface.

The transition from O–Fe–O_3–Fe to O_3–Fe–Fe involves a change in the number of iron atoms at the surface. One possibility consists in the lateral diffusion of iron atoms, for example from steps. Such surface rearrangements are likely to involve complicated kinetic processes and it is quite possible that the O–Fe–O_3–Fe structure is meta-stable for oxygen chemical potentials well above -0.5 eV.

A convenient representation of the results is a plot of the surface free energy as a function of temperature for a given oxygen partial pressure. This is done for a pressure of $P = 0.2$ bar as shown in Fig. 4. At low temperatures, the most stable surface is O_3–Fe–Fe, i.e., a surface fully covered with oxygen atoms. Above approximately 500 K, the O–Fe–O_3–Fe surface is thermodynamically stable. At a temperature of about 850 K, this surface releases oxygen atoms to form the Fe–O_3–Fe surface termination. It is remarkable that the industrial catalyst used in the selective oxidation of ethylbenzene to styrene is operated in this temperature range at comparable oxygen partial pressures. While the

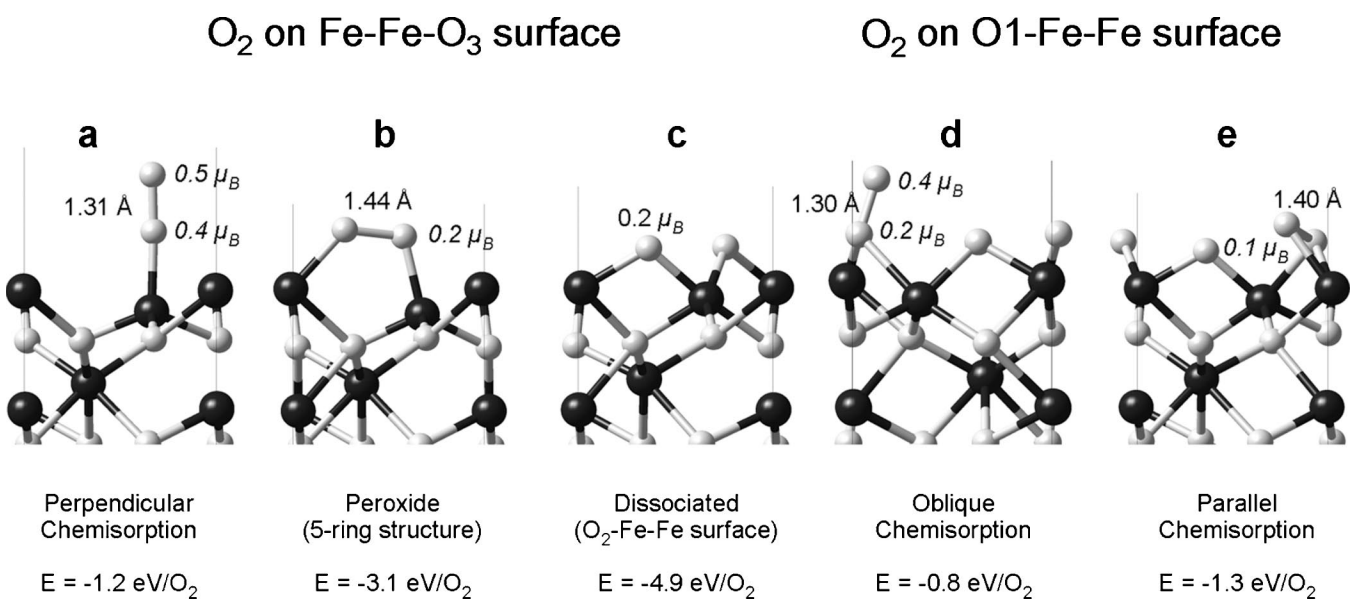

FIG. 5. Chemisorption of an O_2 molecule on the fully reduced Fe–Fe–O_3 surface and desorption from the fully oxidized O_3–Fe–Fe surface. Binding energies, O–O bond distances, and magnetic moments per oxygen atom are given for each geometrical arrangement.

present calculations represent a highly idealized system, the coincidence between the conditions for the release of oxygen from the active surface Fe atoms and the optimal operating conditions for the industrial catalyst could be more than fortuitous.

D. Chemisorption of molecular oxygen on $Fe_2O_3(0001)$ surfaces

In the present context, an important aspect is the interaction of molecular oxygen with the iron oxide surfaces at various levels of oxygen coverage. To this end, we have investigated stable and meta-stable structures of molecular oxygen on $Fe_2O_3(0001)$ surfaces including the regimes of a fully reduced and a fully oxidized surface. Together with the results discussed earlier, a comprehensive picture of the interaction of molecular oxygen with this iron oxide surface is obtained.

As reference, we use the total energy of molecular oxygen O_2 computed in the same cell as used for the surfaces with the same computational parameters. This calculation is spin polarized, since the ground state of the O_2 molecule is a triplet. We obtain an O–O distance of 1.24 Å and a total magnetic moment 2.00 μ_B. The experimental value for the equilibrium bond distance is 1.20752 Å.[22] The overestimation of the bond length by about 3% is somewhat large, but consistent with the typical errors of the GGA. The calculated electronic energy for the O_2 molecule is -9.818 eV, which is the value used in the thermodynamic analysis described earlier.

With the data for the surfaces and molecular O_2, we can create models describing the interaction of oxygen with the surface, compare energies, and we can study the different geometries. Three important cases will be considered, namely (i) the interaction of molecular oxygen with the fully reduced surface Fe–Fe–O_3, (ii) the abstraction of oxygen from the fully oxidized O_3–Fe–Fe surface, and (iii) the interaction with the thermodynamically stable Fe–O_3–Fe surface. In terms of the oxidation state, the latter case falls between a fully reduced and a fully oxidized surface.

1. O_2 on Fe–Fe–O_3 surface

Compared with the O_2–Fe–Fe surface, the separated systems O_2 and Fe–Fe–O_3 are less stable by 4.9 eV per O_2. Thus, the chemisorption of molecular oxygen on the reduced iron oxide surface is strongly exothermic, as expected. Among the many possible configurations of an oxygen molecule binding to this surface, we consider three cases, namely (i) O_2 perpendicular to the surface, (ii) O_2 parallel to the surface, (iii) an oblique angle between the O–O axis and the surface.

In the case of an O_2 molecule constrained to a geometry perpendicular to the surface on top of the lower of the two surface Fe atoms [cf. Fig. 5(a)], we find a chemisorption energy of -1.2 eV per O_2 revealing a strong interaction between the molecule and the surface. Correspondingly, the O–O bond distance increases from 1.24 to 1.31 Å. Upon a slight tilt of the molecule away from the surface, the energy remains almost unchanged. This shows a very flat energy hypersurface for the bending of the oxygen molecule. The chemisorption is accompanied by a reduction of the magnetic moment. As stated earlier, the present calculations correctly give a triplet ground state for the isolated O_2 molecule, i.e., the molecule has a total magnetic moment of 2 μ_B. For the isolated molecule, a projection of the spin density onto spheres around each atom with a radius of 0.82 Å yields a projected moment of 0.8 μ_B per O atom. Upon chemisorption in the perpendicular geometry, this moment is reduced to 0.43 μ_B and 0.50 μ_B per atom for the O atom closer and farther from the surface, respectively. This geometry can be interpreted as an unstable chemisorbed precursor state.

As the angle between the surface and the O–O bond is increased to about 45°, a geometry optimization tilts the molecule further leading to a structure, which could be described as a peroxide [cf. Fig. 5(b)]. In this geometry, the two oxygen atoms form a five-membered ring of –Fe–O–O–Fe–O– and the O–O distance increases to 1.44 Å, which is typical for peroxides. The adsorption energy is -3.1 eV and the projected magnetic moment per O atom is reduced to approximately 0.2 μ_B. This value is close to the magnetic moment of surface oxygen atoms in a fully dissociated form.

In the third case, an O_2 molecule is brought close to the surface in an orientation parallel to the surface. During the geometry optimization, the molecule dissociates, apparently without a barrier, to form an oxygen terminated O_2–Fe–Fe surface. This process gives an energy gain of -4.9 eV per O_2 molecule. In the final geometry, the O atoms have a projected magnetic moment of approximately 0.2 μ_B as in the cases shown in Table IV.

The calculations reveal that on the fully reduced Fe–Fe–O_3 surface, an O_2 molecule dissociates without a kinetic barrier once the molecule achieves a favorable position above the surface. This could be seen as a spontaneous oxidation of the surface. The dependence of the surface energy as a function of the oxygen chemical potential (cf. Fig. 3) shows that over the entire range covered in typical laboratory and reactor conditions, the O_2–Fe–Fe surface is *always* thermodynamically more stable than the Fe–Fe–O_3 surface. From these two results (thermodynamics and kinetics) we can therefore conclude that the Fe–Fe–O_3 surface will not exist under conditions relevant for catalytic processes. In fact, the formation of the Fe–Fe–O_3 surface would require a combination of ultrahigh vacuum and high temperatures, where bulk hematite would start to decompose.

2. O_2 on O_1–Fe–Fe surface

The next case is the fully oxidized O_3–Fe–Fe surface, which can be thought of as the result of the dissociation of O_2 molecules on an O_1–Fe–Fe surface. The O_3–Fe–Fe surface is the most stable termination at very high oxygen partial pressures or very low temperatures. Removal of an O_2 molecule from this surface leads to an O_1–Fe–Fe surface and an O_2 molecule. This process is physically reasonable, because the thermodynamic analysis (cf. Fig. 3) shows that at low oxygen pressures the O_1–Fe–Fe surface is more stable than the fully oxidized surface. For these reasons, we consider the structure and energetics of an O_2 molecule adsorbing on (or desorbing from) an O_1–Fe–Fe surface.

Starting with the O_1–Fe–Fe termination, an O_2 molecule is brought close to the surface and a local minimum is determined by geometry optimizations. Two geometric cases are investigated, namely (i) an O_2 molecule perpendicular to the surface with one of its atoms at the O bulk position of Fe_2O_3, and (ii) a starting geometry with the molecular O–O axis at an angle of approximately 45° with respect to the surface. In both cases the O_2 molecule does not dissociate as was found for O_2 on the fully reduced Fe–Fe–O_3 surface. There are no indications for the formation of a peroxide.

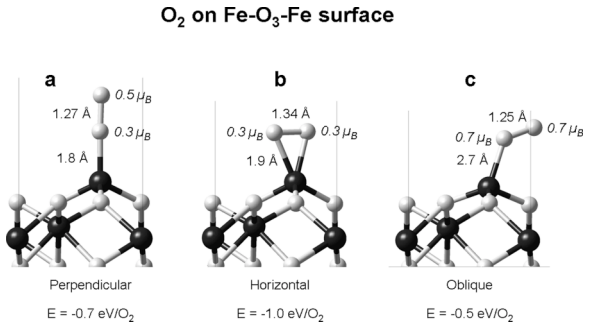

FIG. 6. Chemisorption of an O_2 molecule on the single iron-terminated stoichiometric Fe–O_3–Fe surface. Binding energies, O–O bond distances, and magnetic moments per oxygen atom are given for each geometrical arrangement.

After geometry optimization, the angle between O_2 and the surface is about 30°. Given that the total energy of the fully dissociated state, which corresponds to an O_3–Fe–Fe surface, is 2.9 eV lower than that of the system $O_2 + O_1$–Fe–Fe one has to conclude that there is a barrier for the dissociation and recombination of an O_2 molecule on an O_1–Fe–Fe surface.

The O_2 molecule in an orientation perpendicular to the O_1–Fe–Fe surface shows an adsorption energy of -0.8 eV, which is thermodynamically less stable by 2.1 eV compared to the O_3–Fe–Fe surface. We find a precursor chemisorbed state similar to the above-studied surface, in which the O–O distance is 1.30 Å with magnetic moments of 0.2 and 0.4 μ_B for the corresponding oxygen atoms (the O atom closer to the surface has the lower magnetic moment).

In the case of a starting geometry with an angle of 45° between the O_2 axis and the surface, we obtain a different adsorption geometry with a higher adsorption energy of about -1.3 eV, but no typical peroxide is formed, although the O–O distance is enlarged to 1.40 Å and the angle to the surface is reduced [cf. Fig. 5(e)]. The magnetic moment of the oxygen atoms nearly disappears (less than 0.1 μ_B). With these results we can see that the O_1–Fe–Fe surface corresponds to a local minimum, which could exist under experimental conditions because of the existence of kinetic barriers and the fact that in the surface phase diagram (cf Fig. 3) it is more stable than the O_3–Fe–Fe surface at high temperatures and low oxygen pressures.

3. O on O_3–Fe–Fe surface

The next system probes the regime of highly oxidized iron oxide by investigating the binding of an O atom to one of the three surface oxygen atoms of an O_3–Fe–Fe surface with an O–O distance equivalent to the bond length in an O_2 molecule. One can consider this also as a model of the interaction of an O_2 molecule with an O_2–Fe–Fe surface. In this case, the desorption of O_2 from the O_3–Fe–Fe surface would create one oxygen vacancy. The thermodynamic stability of the systems under investigation (O_3–Fe–Fe $> O_2$–Fe–Fe$+\frac{1}{2}O_2 > O_1$–Fe–Fe$+O_2$, ordered from high to low stability) shows that the reaction O_3–Fe–Fe$+\frac{1}{2}O_2$

$\rightarrow O_2-Fe-Fe+O_2$ constitutes a realistic scenario. In particular, it is of interest if this process of abstracting one oxygen atom from the $O_3-Fe-Fe$ surface involves an energy barrier or not.

To this end, we start from the $O_3-Fe-Fe$ surface, place an additional O atom at about 1.2 Å (i.e., the O_2 bond length) above one of the three surface oxygen atoms and then relax the system. During the geometry optimization, the newly created oxygen molecule tries to escape from the surface. At the resulting minimum, the O atom initially bound to the surface ends up about 0.24 Å higher than the other two surface O atoms. Using this geometry as the starting position for the next calculation, the two O atoms involved in the process of forming an oxygen molecule, i.e., the O_2 molecule itself, are pulled away from the surface in steps of 0.1 Å.

By carrying out this process step-by-step, the energy profile of the desorption (or chemisorption) of an oxygen molecule from (to) an oxidized $Fe_2O_3(0001)$ surface shows no barrier along this path on the energy hypersurface. This would mean that, coming from the gas phase, an O_2 molecule can be adsorbed on the $O_2-Fe-Fe$ surface without a barrier, thus creating an $O_2-O_2-Fe-Fe$ surface, or, in a different notation, an $O_4-Fe-Fe$ termination. This calculation was done with the relaxed $O_4-Fe-Fe$ surface as starting position. In the subsequent removal of the O_2 molecule, the coordinates of the other atoms were frozen. Taking the oxygen chemical potential into consideration, we find that at low temperatures or high oxygen pressures the $O_4-Fe-Fe$ termination is energetically preferred compared to the $O_2-Fe-Fe$ termination.

4. O_2 on $Fe-O_3-Fe$ surface

After the study of the two limiting cases of low and high oxygen coverage, we will now investigate the intermediate thermodynamic conditions corresponding to those found in the typical catalytic oxidation processes with iron oxide catalysts. For instance, the oxidation of ethylbenzene to styrene is carried out at a temperature of about 800 K and a partial oxygen pressure of 0.2 bar. Under these conditions, the thermodynamically most stable surface is the $Fe-O_3-Fe$ surface, which can bind an additional O atom to form the $O-Fe-O_3-Fe$ termination. Here we consider the interaction of an O_2 molecule with the $Fe-O_3-Fe$ surface to form an O_2-Fe-O_3-Fe arrangement. The geometry and stability of this structure is compared with the system O_2+Fe-O_3-Fe.

The following models were taken into consideration (cf. Fig. 6): O_2 perpendicular to the surface [Fig. 6(a)], O_2 parallel to the surface above the surface Fe atom [Fig. 6(b)], and O_2 parallel to the surface between two surface Fe atoms.

The calculations show that for a stoichiometry of one O_2 molecule per surface unit cell, the oxygen molecule is adsorbed parallel to the surface between two Fe atoms in a physisorbed state with an adsorption energy of -0.5 eV per O_2 molecule [Fig. 6(c)]. The O–O distance of 1.25 Å is therefore close to the O_2 bond length of 1.24 Å and the distance to the closest Fe atom is rather large (2.7 Å). The atom-projected magnetic moment of the two O atoms is $0.7\mu_B$, which is only slightly reduced from $0.8\mu_B$ of the free molecule.

A geometry with the O_2 molecule above the surface Fe is energetically more favorable, although neither spontaneous dissociation nor the formation of a peroxide could be observed as was the case for O_2 on the $Fe-Fe-O_3$ surface. This sounds obvious, as in this case the surface is represented by a single Fe atom above the O_3 layer. This Fe atom can form a bond with only one oxygen, whereas the other oxygen would be pushed off by the oxygen layer and should leave the surface after dissociation.

An O_2 molecule bound perpendicularly on top of the surface Fe atom has an adsorption energy of -0.7 eV per molecule, an O–O distance of 1.27 Å, and magnetic moments of $0.3\mu_B$ (the O bound to the Fe atom) and $0.5\mu_B$ of the corresponding O atoms. The most stable geometry occurs when O_2 binds parallel to the Fe atom, with -1.0 eV adsorption energy, 1.34 Å O–O distance, and magnetic moments of $0.3\ \mu_B$ for each of the two O atoms. The O–Fe distance is 1.8 Å in the perpendicular arrangement and 1.9 Å in the parallel geometry.

VI. SUMMARY AND CONCLUSIONS

Spin-polarized *ab initio* DFT-GGA calculations using PAW potentials as implemented in VASP have been used to investigate the structure and thermodynamic stability of the (0001) surfaces of Fe_2O_3 (hematite). For high chemical potentials of oxygen, i.e., at a high oxygen partial pressure and at low temperature, the most stable (0001) surface of hematite is completely covered with oxygen atoms. This termination is denoted $O_3-Fe-Fe$ surface. At low oxygen chemical potentials, but within the stability range of bulk hematite, the (0001) surface is terminated by an oxygen layer with one iron atom per two-dimensional unit cell slightly above the plane of the surface oxygen atoms. This case is denoted as $Fe-O_3-Fe$ surface and corresponds to a fully stoichiometric surface with the surface atoms in the formal oxidation state of $+3$. The fully reduced form, which would be terminated solely with Fe atoms, is thermodynamically unstable. In fact, this surface is found to be highly reactive, as it dissociates adsorbed oxygen molecules spontaneously.

In the regime of intermediate values of the oxygen chemical potential, two surface structures have very similar stability, namely $Fe-O_3-Fe$, which is terminated by Fe atoms, and $O-Fe-O_3-Fe$, where an additional oxygen atom is attached to the surface Fe atoms. In this case, the formal oxidation state of the surface Fe atoms is $+5$ and one can refer to this case as ferrate-like structure, since the tetrahedral coordination of Fe(V) in this surface termination is similar to that in ferrates such as $K_3(FeO_4)$.

Thus, the surface $Fe-O_3-Fe$ has the ability to accept and release oxygen upon small changes in the chemical potential of oxygen. For a pressure of 0.2 bar, the cross-over between the surfaces with and without the attached oxygen is at a temperature of about 850 K. It is probably not a coincidence that the oxidation of ethylbenzene to styrene using an iron oxide catalyst is carried out in this temperature and pressure range.

Computations describing the interaction of molecular oxygen with (0001) surfaces of hematite reveal that the completely reduced surface (i.e., a surface terminated solely by Fe atoms) would dissociate O_2 molecules spontaneously. Such a behavior is not found for surfaces such as $O_1-Fe-Fe$, which are already partially oxidized before the addition of O_2 molecules.

At this point, it behooves us to assess the uncertainties of the present computational study. Assuming that crystallographically perfect surfaces are representative models, the dominant uncertainty in the present predictions of the structural and chemical properties of iron oxide surfaces comes from the use of the GGA-DFT. One could argue that this level of approximation is inadequate for describing the electronic structure of strongly correlated systems such as iron oxides. In particular, there are serious concerns about the correct ordering of O-p vs. Fe-d states near the Fermi level.[23] Errors of this kind could change the nature of the frontier orbitals and thus lead to an incorrect description of the chemical bonding.

In order to probe the validity of the GGA-DFT approach, we have performed computations for the bulk crystals FeO and Fe_2O_3 as well as for the isolated FeO molecule. In terms of coordination number and chemical environment, surfaces lie between these two extremes. These test calculations show that equilibrium bond distances as well as magnetic moments for the bulk crystals and the FeO molecule are quite well described on the GGA-DFT level of theory and that the deviation between computed and experimental values is very similar to those found for many other systems. This implies that properties such as the total energy or total densities, which depend on integrals over the space and energy spectrum, are reasonably well described by the GGA-DFT level of theory, even if details around the Fermi energy may not be properly accounted for. While it is reasonable to expect that the key structural and thermochemical features of iron oxide surfaces are captured by the current computations, the validity of the present approach will have to be proven by experiment. To this end, the thermodynamic analysis of the transition between the structures denoted $Fe-O_3-Fe$ and $O-Fe-O_3-Fe$ provides a critical test.

Other uncertainties in the present study originate from the use of a finite slab to represent the surface. Experience with other systems shows that a thickness of approximately 12 layers should be sufficient to describe the structure and energetics of surfaces. Furthermore, the slabs are constructed in such a way that they do not exhibit a dipole moment. This construction prevents errors due to spurious long-range interactions between the slabs in the supercell approach. A further possible source of uncertainty in the predicted structures comes from the fact that all models used in the present study have the same periodicity in the directions parallel to the (0001) surface as the conventional hexagonal unit cell of a corundum structures. In other words, no surface reconstructions are considered. Another source of uncertainty comes from the neglect of the temperature dependent vibrational parts of the free energy and entropy of bulk and surface calculations. Furthermore, the present model does not consider configurational contributions to the entropy. Although the electronic energy presents the dominant component of the internal energy, the vibrational and configurational contributions could have significant consequences. Finally, it is possible that energy minimizations using conjugate gradient methods miss relevant minima on the energy hypersurface. In the present systems, this could occur for structures which involve a major rearrangement of atoms throughout several layers near the surface. While such scenarios cannot be excluded, it is believed that through the systematic exploration of a range of different oxygen coverages, as was done in the present study, the key surfaces structures have been addressed.

ACKNOWLEDGMENTS

Fruitful discussions with Professor J. Hafner and Professor G. Kresse are gratefully acknowledged. This work was supported by the European Commission within its *Training and Mobility of Researchers* Program under Contract No. ERB FRMX CT 98-0178.

*Corresponding author. Email address: ewimmer@materialsdesign.com

[1] P. Hohenberg and W. Kohn, Phys. Rev. **136**, B864 (1964).
[2] W. Kohn and L. J. Sham, Phys. Rev. **140**, A1133 (1965).
[3] O. Gunnarsson, B. I. Lundqvist, and S. Lundqvist, Solid State Commun. **11**, 149 (1972).
[4] U. von Barth and L. Hedin, J. Phys. C **5**, 1629 (1972).
[5] Y. Wang and J. P. Perdew, Phys. Rev. B **44**, 13298 (1991).
[6] J. P. Perdew, J. A. Chevary, S. H. Vosko, K. A. Jackson, M. R. Pederson, D. J. Singh, and C. Fiolhais, Phys. Rev. B **46**, 6671 (1992).
[7] G. Kresse and J. Hafner, Phys. Rev. B **47**, 558 (1993).
[8] G. Kresse and J. Furthmüller, Phys. Rev. B **54**, 11169 (1996).
[9] G. Kresse and J. Furthmüller, Comput. Mater. Sci. **6**, 15 (1996).
[10] P. E. Blöchl, Phys. Rev. B **50**, 17953 (1994).
[11] G. Kresse and J. Joubert, Phys. Rev. B **59**, 1758 (1999).
[12] X.-G. Wang, W. Weiss, Sh. K. Shaikhutdinov, M. Ritter, M. Petersen, F. Wagner, R. Schlögel, and M. Scheffler, Phys. Rev. Lett. **81**, 1038 (1998).
[13] W. Weiss and W. Ranke, Surf. Sci. **70**, 1 (2002).
[14] A. Zangwill, *Physics of Surfaces* (Cambridge University Press, New York, 1988).
[15] D. R. Stull and H. Prophet, *JANAF Thermochemical Tables*, 2nd ed. (U.S. National Bureau of Standards, Washington, DC, 1971).
[16] Th. Schedel-Niedrig, W. Weiss, and R. Schlögl, Phys. Rev. B **52**, 17449 (1995).
[17] W. Weiss, Surf. Sci. **377**, 943 (1997).
[18] MedeA 1.7, Materials Design, Inc., Angel Fire, NM, 2002.
[19] M. Akimitsu, T. Mizoguchi, J. Akimitsu, and S. Kimura, J. Phys. Chem. Solids **44**, 497 (1983).
[20] P. C. Engelking and W. C. Lineberger, J. Chem. Phys. **66**, 5054 (1977).
[21] P. S. Bagus and H. J. T. Preston, J. Chem. Phys. **59**, 2986 (1973).
[22] K. P. Huber and G. Herzberg, *Constants of Diatomic Molecules* (data prepared by J. W. Gallagher and R. D. Johnson, III) in *NIST Chemistry WebBook, NIST Standard Reference Database*

Number 69, edited by P. J. Linstrom and W. G. Mallard, March 2003, National Institute of Standards and Technology, Gaithersburg MD, 20899 (http://webbook.nist.gov).
[23] J. Hafner (private communication).
[24] S. Surnev, G. Kresse, M. Sock, M. G. Ramsey, and F. P. Netzer, Surf. Sci. **495**, 91 (2001).
[25] K. Mader and R. Hoppe, Z. Anorg. Allg. Chem. **586**, 115 (1990) as found in the Inorganic Crystal Structure Database (ICSD) of the Fachinformationszentrum Karlruhe, Germany.